

Effect of Chemical Treatment on Silicon Manganese: Its Morphological, Elemental and Spectral Properties and Its Usage in Concrete

Chin Mei Yun

Swinburne University of Technology - Sarawak Campus

Muhammad Khusairy Bin Bakri (✉ kucaigila@yahoo.com)

Universiti Malaysia Sarawak <https://orcid.org/0000-0003-1971-2350>

Md Rezaur Rahman

Universiti Malaysia Sarawak

Kuok King Kuok

Swinburne University of Technology - Sarawak Campus

Perry Law Nyuk Khui



Universiti Malaysia Sarawak

Research Article

Keywords: Silicon, Manganese, Modification, Characterization, Applications, Concrete

Posted Date: October 19th, 2021

DOI: <https://doi.org/10.21203/rs.3.rs-957374/v1>

License:   This work is licensed under a Creative Commons Attribution 4.0 International License. [Read Full License](#)

Version of Record: A version of this preprint was published at Silicon on January 7th, 2022. See the published version at <https://doi.org/10.1007/s12633-021-01569-4>.

Abstract

The effect of chemical treatment on silicon manganese slag and the effect of curing time on the compressive strength of completely replacement coarse aggregate silicon manganese concrete (SMC) relative to normal weight concrete (NWC) with gravel as coarse aggregate is the subject of this paper. Alkali and acidic base chemicals are used to alter the neat silicon manganese slag during chemical preparation. The mixture pattern proportions for Grade 30 and Grade 50, respectively, were used to create the concrete. Before the compressive strength tests, the samples were cast and cured for 7-, 14-, and 28-days. The properties of the silicon manganese slag and its concrete were studied using a scanning electron microscope (SEM), energy dispersive x-ray spectroscopy (EDS), and Fourier transform infrared spectroscopy (FTIR). The compressive pressure of SMC30 and SMC50 obtained were 37.3 MPa and 51.1 MPa, respectively, on the 28-day. The alkaline treatment smoothes the matrix, while the acid treatment roughens the composition of the silicon manganese slag, according to SEM. The functional group demonstrated a major improvement in FTIR, while EDS revealed a high content of both silicon (Si) and manganese (Mn) elements. As a result, it can be observed that the power of SMC increases as the curing time increases for samples with complete replacement of normal aggregates using silicon slag

1.0 Introduction

It has become more popular in the construction of many high-rise buildings due to the vast growth in every country worldwide, particularly in the big city, which emphasized the conservation and sustainability against the environment [1–6]. These high-rise buildings play an important role in housing the communities, while minimizing environmental impact [1–6]. The lightweight concrete structural, which uses either natural or artificial lightweight aggregates [7], is commonly used in these high-rise structures, which are made up of a combination of heavyweight and lightweight materials. Through lighter weight of construction materials used in massive self-weight structures, a low weight unit of lightweight structural concrete has been produced [1–6]. Many scarce natural lightweight materials, such as shale, limestone, and sand, may be conserved with the increment usage as construction materials, hence artificial lightweight aggregates are source as alternative replacement [8–10]. However, it was top developed and emerging countries such as China, Russia, India, Korea, Japan, the United States, and Australia that contributed to technical understanding on the use of artificial aggregates. Malaysia is only a few years behind the rest of the world in terms of technological innovation [11, 12]. Despite the current environmental damage and aggregate source depletion problems, there is little research on aggregate use and development as a substitute for natural lightweight by using artificial aggregates, especially in Malaysia [13].

Using the example of one of the most popular and effective byproducts in the world, bottom and fly ash as a combusted inorganic material, which is considered to be used as artificial lightweight aggregates from raw material due to its volume expansion stability [14–16]. However, greenhouse gases are highly created and extracted by thermal power plants where a significant amount of energy is required, which is expensive, as the production of artificial lightweight aggregates may require a sintering process at 900–1300°C, which is typically combined with an inorganic material [17]. To address these issues, various studies have been performed using physical non-sintering coal ash processing processes, such as generating aggregates by mixing with binders [18–20].

Apart from blast furnace slag, which was traditionally used as a concrete admixture, most slags produced in the steel, iron, or metal industries have no applications due to their extraction process and technique [21]. However, owing to underdevelopment and a lack of research information on the usage of blast furnace slags in Malaysia, these slags are simply thrown away in the landfill as waste [22]. The lack of awareness and misinterpretation that most slags generated contain significant amounts of iron oxides (Fe-oxides), free-calcium oxide (free-CaO), and free-magnesium

oxide (free-MgO) may explain the lack of information toward the application [23]. The majority of these free-CaO and -MgO can form during slow cooling, while the amorphous phase forms during rapid cooling, and the high-temperature molten slag has an amorphous structure until cooling [24–26]. Despite their Fe-based hydroxides, $\text{Mg}(\text{OH})_2$, and $\text{Ca}(\text{OH})_2$ forms, the majority of these compounds extend as they come into contact with water [27–29]. Furthermore, most steel slags produced had high thermal conductivity and net mass, making them unsuitable for use in normal-weight concrete. Slags are not used as by-products as fillers, binders, or aggregates for concrete in Malaysia, and have never been used as raw materials for any artificial lightweight aggregates. The Malaysian Standard (MS) and the Works Department (WD) do not have it completely registered and standardized. Furthermore, the Department of Environment (DOE) classifies it as a schedule waste. As a result, extensive research is needed to determine the most suitable use of slags as a building material.

A nonferrous metal, silicon manganese (SiMn) slag, is produced during the smelting process. It contains a lot of Si-based oxide and a little Fe-based oxide. Frias et al. [30] identified a fine SiMn slag powder suitable for use as aggregate in concrete, which improves volumetric and thermal stability when used as a cement admixture [31–32]. The molten SiMn slag induces water evaporation when it comes into contact with water due to its high thermal temperature, which created small pores on the inner layer of the slag and large pores on the outer slag layer as the cooling process progressed. Since the pore formation could intimidate an important lightweight aggregates resource, it has a lot of potential for commercialization in construction and building materials, particularly in Malaysia.

The three most popular cooling methods are (i) air cooling, (ii) water cooling (by quenching), and (iii) compound quenching (by oil, chemical aqueous solution, etc.). Furthermore, slow cooling by air-cooled by leaving the slag in an open storage until it cooled for a certain time, if sprinkling occurred, either through water, etc., can have a variety of effects on the slag's consistency, with dust, restricted open storage, and leachate generation all contributing to the issues [33]. Furthermore, most molten SiMn slag in Malaysia are condensed, solidified as big rocks, and deposited as waste in landfills, while it needed to be compressed to be used as coarse aggregate. This results in a rise in waste in the landfill's small capacity.

In this paper, the potentials of SiMn slag aggregates are reported, in which SiMn slag aggregates were studied using alkali, acid, and heat treatment in this analysis. To describe and analyses the effect of chemical and heat alteration on SiMn slag, limestone, Ordinary Portland Cement (OPC), and Silicon Manganese Concrete, scanning electron microscopy (SEM), energy dispersive x-ray spectroscopy (EDX/EDS), and Fourier transform infrared spectroscopy (FTIR) are used (SMC). A fundamental research was also carried out to compare and measure the usability of SiMn Slag Manganese Concrete (SMC) as standard concrete aggregates with OPC. The concrete's compressive strength was compared to that of Normal Weight Concrete (NWC), and the compression strength properties of both were investigated and documented.

2.0 Methodology

2.1 MATERIALS

Silicon manganese slag (SiMn slag) was obtained from OM Materials Sdn. Bhd., Bintulu, Sarawak, Malaysia. Ordinary Portland cement (OPC) were obtained from Cahaya Mata Sarawak (CMS) Berhad. Kuching, Sarawak, Malaysia. Crushed aggregates as coarse aggregates for NWC and river sand as fine aggregates for both NWC and SMC were obtained locally from Sarawak. Plasticizing REAL FLOW 671 admixture cement was supplied by Real Point Sdn. Bhd, Selangor Malaysia. For chemical treatment, sodium hydroxide, NaOH (alkaline) (CAS 1310-73-2), hydrochloric acid, HCl (acidic) (CAS 7647-01-0), sulfuric acid, H_2SO_4 (acidic acid) (CAS 7664-93-9) were used. These inorganic chemicals

were supplied by Fisher Scientific International, Inc. from United States. The caustic soda of NaOH obtained is industrially produced through electrolytic chloralkaline process. It is dissolves in water to form a colorless solution. HCl obtained is in aqueous form captured from hydrogen chloride gas. It is soluble in water and alcohol, clear and colorless liquid with strong pungent smell, which act as reagent for samples. H₂SO₄ is formed naturally oxidation of sulfide mineral. It also commercially produced when sulfur trioxide is dissolved in water.

2.2 METHODOLOGY

2.2.1 SILICON MANGANESE SLAG CHEMICAL TREATMENT

The obtained silicon manganese, SiMn slag was divided into 4 categories: Neat-SiMn, NaOH-SiMn, HCl-SiMn, H₂SO₄-SiMn. For chemical treatment, solution was created by mixing 5wt% of caustic soda of NaOH with 95wt% of distilled water to prepare NaOH solution, 5wt% aqueous of HCl with 95wt% of distilled water to prepare HCl solution, 5wt% aqueous of H₂SO₄ with 95wt% of distilled water to prepare H₂SO₄ solution. The solid SiMn was crunch into 10mm size and soaked in each of the chemical solution to create modified NaOH-SiMn, HCl-SiMn, and H₂SO₄-SiMn for 15 minutes before filtered and dry for heat treatment in an open-ventilated drying oven for 30 minutes under temperature of 90°C.

2.2.2 CONCRETE MIXTURE PROPORTIONS

The mixture proportions design is shown in Table 1. It was design to achieved concrete compressive strength of Grade 30 and 50 MPa, respectively. Silicon manganese slag was used as coarse aggregates for SMC. Meanwhile, for NWC, gravel was used as the coarse aggregates. Both samples, NWC and SMC used 20 mm size coarse aggregates. For the fine aggregates, river sand was used. The admixture used has an admixture of high-range water-reducing and set-retarding for concrete, which complied with Type B, D and G of ASTM C494-19 [34] and BS 5075-1:1982 [35]. The specifications and the amount were shown in Table 1 for each concrete type.

Table 1
The Mixture Proportions for NWC and SMC.

Mix Proportions by Weight (kg/m ³)	NWC30	NWC50	SMC30	SMC50
Cement	360	500	360	500
Fine Aggregate	730	710	730	710
Coarse Aggregate	1100	1040	1100	1040
Water	166	168	166	168
Admixture (ml)	2880 ml	5500ml	2880 ml	5500ml
Water to binder ratio	0.46	0.34	0.46	0.34

2.2.3 Concrete Preparation

For each batch of concrete, nine samples of concrete cubes were prepared. The samples were cast, cured and tested on the 7-day, 14-day, and 28-day, respectively. During the cast for NWC30 and NWC50, natural river sand and crushed aggregates was used for fine and coarse aggregate, respectively. While for SMC30 and SMC50, natural sand and silicon manganese slag was used for fine and coarse aggregates, respectively. The samples were mixed using concrete mixing drum according to mixture proportions shown in Table 1. Water with respect to water to binder ratio shown in Table 1 was added into the concrete mixture, and the concrete were mixed thoroughly for 15 minutes. The concrete mixture was then placed into the concrete steel cube molds of 150 mm X 150 mm X 150 mm with 3 equal layers of compaction applied. Compaction was carried out using vibration table to remove the entrapped air and to

avoid segregation of particles. Subsequently, the concrete mixture in the steel cube molds were left to dry in the lab for 24 hours before demolding were carried out. The samples were then placed in water tank filled with water, which cured up to 7 days, 14 days, and 28 days prior to compressive test. The procedures of casting and curing is in accordance the IS 10262:2019 standard [36].

2.2.4 Characterization and Testing

2.2.4.1 SEM and EDX/EDS Analysis

ASTM E2015-04 [37], ASTM E2142-08 [38], and ASTM C1723-16 [39] standards were used to perform scanning electron microscopy (SEM) with energy dispersive x-ray spectroscopy (EDX/EDS). A magnification of 500x was used to examine a variety of SiMn slag, granite, and ordinary Portland cement samples, as well as their concrete. Furthermore, EDX/EDS was performed in accordance with ASTM E1508-12 [40]. Three points were chosen at random from the neat and modified SiMn slag, limestone, Portland cement, and concrete samples. The elemental composition percentages analysis was automated by the program. The EDX/EDS was replicated several times for each study, and the most common findings were carefully selected. For the SEM and EDX/EDS, A Hitachi TM4000Plus Tabletop Microscope with a Quantax75TM Series Energy Dispersive X-Ray Spectrometer (Hitachi Ltd., Tokyo, Japan) was used to analyses the neat and modified SiMn, limestone, ordinary Portland cement, and silicon manganese concrete (SMC) samples to investigate its composition, size and surface structure.

2.2.4.2 FTIR Analysis

A Fourier-transform infrared spectroscopy (IRAffinity⁻¹, Shimadzu Corporation, Kyoto, Japan) was used for the FTIR analysis of the neat and modified SiMn slag, limestone, ordinary Portland cement, and SiMn slag aggregate concrete (SMC) samples for comparison. Fourier-transform infrared spectroscopy was conducted according to the ASTM E168-16 [41] and ASTM E1252-98 [42] standards for qualitative and quantitative analysis. The spectrum scanning was conducted in the wavenumber range of 4000 cm⁻¹ to 400 cm⁻¹ for each sample. Fourier-transform infrared spectroscopy utilized the infrared spectrum transmittance and absorption of the samples to develop a unique molecular fingerprint spectrum. The test was repeated numerous times for each sample, and the most representative results were selected.

2.2.4.3 Compressive Test

On the testing day, the concrete samples were removed from the water tank and the compressive strength test was conducted in accordance with BS EN 196-1:2016 [43] using the electrically operated U20CrEL Model of Motorized Hydraulic Compression Testing Machine. During the compressive test, load was applied gradually on top of the concrete samples at 2.4 ± 0.2 kN/s, until the samples failed. Results obtained from the same three concrete batch samples of on same testing days with respect to 7-, 14- and 28-days were averaged and reported.

3.0 Results And Discussions

3.1 Compressive Strength

Figure 1 shows the compressive strength of NWC and SMC with full replacements of gravels using silicon manganese slag at 7-, 14- and 28-days. For both NWC and SMC, the compressive strength increases with the curing duration. Although SMC samples had shown slightly lower compressive strength compared to NWC at all curing period, SMC30 and SMC50 achieved compressive strength of 37.3 MPa and 51.1 MPa at the 28-days, which passed Grade 30 and Grade 50 mixture design proportion standards. At the 7-days, SMC30 demonstrate 6.3% compressive strength

reduction compared to NWC30 whilst SMC50 achieve 10% compressive strength lesser than NWC50. At the 14-days, SMC30 achieve comparable compressive strength with NWC30 while SMC50 demonstrate 16% compressive strength reduction compared to NWC50. While at the 28-days, SMC30 and NWC30 displayed comparable compressive strength. However, SMC50 shown 9.2% compressive strength reduction compared to NWC50.

It was observed that both NWC and SMC samples had surpassed the typical specified compressive strength for structural application of 30 MPa and 50 MPa. Ganesh et al. [44] found a similar result for Grade 30 concrete, where the complete substitution of coarse aggregates with silicon manganese slag reached 30.44 MPa at the 28-day with a slightly lower cement content of 330 kg/m³ and a slightly lower cement content of 330 kg/m³.

3.2 MORPHOLOGICAL ANALYSIS

SEM photographs of limestone, ordinary Portland cement, and silicon manganese slag aggregate concrete are seen in Figure 2 (a), (b), and (c) at 500x magnification (SMC). Figure 2 (a) depicts a limestone sample aggregate that was used in architecture, housing, paving, and road materials in Sarawak, Malaysia. According to the samples, the limestone is brittle mosaic in surface structures of inconsistent grain size, with some having small soft bit structures that vary in form and grove [45–48]. Many researchers [49] have stated that the brittle and inconsistently sized, shapes, groove surface structures, and poor hydration of limestone can cause weak adhesion at certain parts of the concrete and composites, particularly when bonded with polymer, bitumen, or cement. Initial cracks may occur before or after the limestone has been bonded, particularly when the materials are loaded [49]. When a load is added to the components, this results in a random breaking point at a certain region of the threshold [49].

The ordinary Portland cement without admixture is seen in Figure 2 (b). The hydration process was irregular, as there was a combination of un-hydrated and hydrated cement in some areas, resulting in a small size crack on the cement surface [50]. In contrast, Figure 2 (c) depicts a slight crack between the silicon manganese slag and ordinary Portland cement used by SMC. The smooth surface of silicon manganese slag slipped, transferred, or moved due to the load added to it during the compressive strength test, which was also a typical failure in many forms of concrete [50–52]. It is also worth noting that for SMC, the interaction between sand and other materials is correctly combined, resulting in better samples.

Figure 3 (a), (b), (c), and (d) reveal images of Neat-SiMn, NaOH-SiMn, HCl-SiMn, and H₂SO₄-SiMn slag at 500x magnification. The alkaline treatment results in a smoother surface with less grain, as seen in Figure 3 (b), while the acidic treatment results in porosity on the surface of the silicon manganese slag, as seen in Figure 3 (c) and Figure 3 (d). It was also discovered that different chemical compositions and concentrations on the surface of the silicon manganese slag produce different reactions. The acid concentration and composition in Figure 3 (d) appear to produce a special needle fascinated shape, resulting in a rougher and more readily absorbent surface [53]. When comparing Figures 3 (c) and 3 (d), it can be shown that the acidic concentration and composition appear to eliminate unwanted weak structures, resulting in a small amount of porous structure on the surface [53].

3.3 EDX/EDS Analysis

Table 1, Table 2 and Table 3 shows the EDS/EDX elemental analyses for limestone, ordinary Portland cement, and silicon manganese concrete (SMC). Figure 4, Figure 5, and Figure 6 depicted the graph continuum of Table 2, Table 3 and Table 4 correlation results, respectively. Carbon (C), oxygen (O), calcium (Ca), natrium (Na), and chlorine (Cl) were found in the samples, according to Table 2. Table 3 shows the presence of carbon (C), calcium (Ca), oxygen (O), silicon (Si), potassium (K), natrium (Na), chlorine (Cl), and aluminium (Al) throughout the samples. Figures 4 and 5 and Tables 2 and 3 indicate that oxygen has the largest mass percentage, followed by calcium and carbon, while other elements have low mass percentages. This shows that limestone contained mostly CaCO₃, CaO, Na₂O, and slight amount of

NaCl [54]. While ordinary Portland cement contained mostly CaCO_3 , CaO , SiO_2 , Al_2O_3 , Na_2O , K_2O , and slight amount of NaCl [55–57]. The present of CaCO_3 and CaO helps strengthen and increase the durability of the limestone and ordinary Portland cement, which also accelerate the effect of hydration reactivity rate [58]. However, the present of slight NaCl may promote corrosion towards steel in concrete, which make it weaker in long period [59–60]

In silicon manganese concrete, as shown in Table 4, the present element in the samples were calcium (Ca), oxygen (O), silicon (Si), carbon (C), aluminium (Al), manganese (Mn), barium (Ba), magnesium, (Mg), natrium (Na), and potassium (K). From Figure 6 and Table 4, it showed that oxygen had the highest content mass percentage, followed by calcium and silicon, while the other elements mass percentage remain low. This shows that silicon manganese concrete contained mostly CaCO_3 , CaO , Na_2O , SiO_2 , Al_2O_3 , Na_2O , K_2O , BaO , BaCO_3 , MgO , SiMn , MnO [4, 32]. The present of CaCO_3 and CaO helps strengthen concrete, and accelerate the effect of hydration rate, while BaO , and BaCO_3 increase the dense of the concrete [58, 32]. However, the absence of NaCl, especially chlorine, reduced corrosion effects towards steel in concrete, which could retain its strength in long period [4, 61, 62]

Table 2
EDS element composition for limestone

Element	Atomic No.	Mass Normal (%)	Atom (%)	Absolute Error (%) (1 sigma)	Relative Error (%) (1 sigma)
O	8	47.05	54.89	6.78	12.52
Ca	20	33.59	15.64	1.18	3.05
C	6	18.62	28.94	2.83	13.22
Na	11	0.50	0.41	0.07	12.07
Cl	17	0.24	0.12	0.04	14.15
Total		100	100		

Table 3
EDS element composition for ordinary Portland cement

Element	Atomic No.	Mass Normal (%)	Atom (%)	Absolute Error (%) (1 sigma)	Relative Error (%) (1 sigma)
O	8	41.72	48.86	5.72	12.82
Ca	20	32.51	15.20	1.07	3.06
C	6	21.15	33.00	3.01	13.31
Si	14	1.97	1.31	0.12	5.57
K	19	1.01	0.48	0.06	5.91
Na	11	0.79	0.64	0.09	10.19
Cl	17	0.51	0.27	0.05	8.69
Al	13	0.34	0.24	0.05	12.74
Total		100	100		

Table 4
EDS element composition for silicon manganese cement (SMC).

Element	Atomic No.	Mass Normal (%)	Atom (%)	Absolute Error (%) (1 sigma)	Relative Error (%) (1 sigma)
O	8	46.33	63.38	4.29	12.67
Ca	20	29.35	16.03	0.67	3.12
Si	14	10.63	8.28	0.35	4.53
C	6	3.65	6.60	0.58	22.04
Al	13	3.36	2.73	0.14	5.85
Mn	25	2.93	1.17	0.10	4.85
Ba	56	1.75	0.28	0.08	5.89
Mg	12	1.07	0.97	0.07	9.18
K	19	0.70	0.39	0.05	8.91
Na	11	0.25	0.17	0.03	19.09
Total		100	100		

The EDS/EDX elemental analysis for Neat-SiMn, NaOH-SiMn, HCl-SiMn and H₂SO₄-SiMn slag are shown in Table 5, Table 6, Table 7, and Table 8. While Figure 7, Figure 8, Figure 9 and Figure 10 showed the graph spectrum correlation with data in Table 5, Table 6, Table 7, and Table 8, respectively. Based on Table 5, Table 6, Table 7 and Table 8, similar present element in all the samples were calcium (Ca), oxygen (O), silicon (Si), carbon (C), potassium (K), barium (Ba), and aluminium (Al). It is also noted that in the Neat-SiMn, NaOH-SiMn, and HCl-SiMn, there is a present of manganese (Mn), magnesium (Mg), and natrium (Na), even though it is not present in H₂SO₄-SiMn. NaOH treatment cause the present of nitrogen (N) in NaOH-SiMn, while HCl cause the present of chlorine (Cl) and lead (Pb), and H₂SO₄-SiMn cause the present of sulphur (S). From Figure 7, Figure 8, Figure 9 and Figure 10, and Table 5, Table 6, Table 7 and Table 8, it showed that the highest content was oxygen mass percentage, while other elements mass percentage remain low. This shows that Neat-SiMn slag contained mostly CaCO₃, CaO, Na₂O, SiMn, Al₂O₃, BaO, BaCO₃, Na₂O, K₂O, SiO, SiO₂, and MgO [4, 32, 63–65]. While BaO, and BaCO₃ increase the density, CaCO₃ and CaO helps to strengthen by increasing the durability of silicon manganese slag, by accelerating the hydration reactivity rate [58, 32]. The present of SiO and SiO₂ created mixture of crystalline and amorphous structure, depending on the chemical reaction towards the chemical treatments, which was reflected in SEM result in Figure 3.

Table 5
EDS element composition for Neat-SiMn

Element	Atomic No.	Mass Normal (%)	Atom (%)	Absolute Error (%) (1 sigma)	Relative Error (%) (1 sigma)
O	8	44.63	55.73	6.36	12.18
Si	14	13.18	9.37	0.67	4.36
C	6	11.70	19.47	2.25	16.40
Ca	20	10.81	5.39	0.41	3.25
Al	13	6.77	5.01	0.40	5.04
Ba	56	5.18	0.75	0.22	3.63
Mn	25	4.03	1.47	0.18	3.91
Mg	12	2.34	1.92	0.18	6.52
K	19	0.82	0.42	0.06	6.48
Na	11	0.53	0.46	0.07	11.80
Total		100	100		

Table 6
EDS element composition for NaOH-SiMn

Element	Atomic No.	Mass Normal (%)	Atom (%)	Absolute Error (%) (1 sigma)	Relative Error (%) (1 sigma)
O	8	47.05	57.21	7.26	12.07
Si	14	13.51	9.36	0.75	4.34
C	6	10.13	16.41	2.17	16.77
Ca	20	10.09	4.90	0.42	3.25
Al	13	5.99	4.32	0.39	5.06
Mn	25	4.15	1.47	0.20	3.83
Ba	56	2.81	0.40	0.15	4.14
Mg	12	2.49	1.99	0.20	6.36
N	7	1.93	2.68	0.68	27.66
Na	11	0.99	0.84	0.11	9.09
K	19	0.87	0.43	0.07	6.06
Total		100	100		

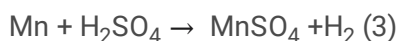
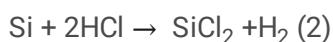
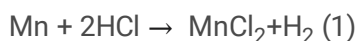
Table 7
EDS element composition for HCl-SiMn

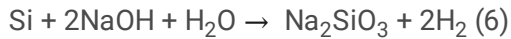
Element	Atomic No.	Mass Normal (%)	Atom (%)	Absolute Error (%) (1 sigma)	Relative Error (%) (1 sigma)
O	8	42.09	58.62	4.13	12.36
Si	14	13.39	10.62	0.47	4.44
Ca	20	11.27	6.27	0.30	3.35
Ba	56	10.90	1.77	0.29	3.36
Al	13	7.62	6.29	0.31	5.14
C	6	6.21	11.52	0.98	19.94
Mn	25	4.49	1.82	0.15	4.16
Mg	12	1.44	1.32	0.09	8.05
Cl	17	1.01	0.64	0.06	7.12
K	19	1.00	0.57	0.06	6.99
Na	11	0.58	0.56	0.06	13.25
Pb	82	0.00	0.00	0.00	1.51
Total		100	100		

Table 8
EDS element composition for H₂SO₄-SiMn

Element	Atomic No.	Mass Normal (%)	Atom (%)	Absolute Error (%) (1 sigma)	Relative Error (%) (1 sigma)
O	8	56.54	71.56	7.53	11.96
Ca	20	14.88	7.52	0.53	3.19
S	16	11.08	6.99	0.47	3.78
Ba	56	7.30	1.08	0.28	3.44
C	6	5.75	9.69	1.25	19.46
Si	14	2.19	1.58	0.13	5.43
Al	13	1.79	1.34	0.12	6.23
K	19	0.48	0.25	0.05	9.10
Total		100	100		

From the analysis it is noted that there are few possible chemical reactions happened during the treatments. Equation (1) to (6) shows the possibilities of the chemical reactions.





3.4 FTIR ANALYSIS

Figure 11, Figure 12, and Figure 13 shows the FTIR images for limestone, ordinary Portland cement and silicon manganese concrete. According to Figure 13, the broad band intensity of 3500 cm^{-1} - 3000 cm^{-1} designated to the water molecules, which is due to stretching of-OH and vibrations of H-O-H. The small sharp peaks in Figure 11 at 3940 cm^{-1} , 3817 cm^{-1} , 3745 cm^{-1} and Figure 12 at 3739 cm^{-1} was due to the free hydroxyl groups. This free hydroxyl group tend to react during hydraulic hydration process. The reaction caused the surface materials entrapped in cavities or void in the polymeric framework. In Figure 11, Figure 12, and Figure 13, few small sharp peaks spotted throughout the 2520 to 1037 cm^{-1} , 2453 to 866 cm^{-1} , 2520 to 690 cm^{-1} , absorption band was designated to the calcium in the form of calcite (CaCO_3) [66-68]. Whereas most CO_3^{2-} having asymmetric stretching, in-plane and out-of-plane bending [69]. In Figure 13, at 1425 and 999 cm^{-1} , the peak was designated for asymmetric stretching and vibration of Si-O-Al and/or Si-O-Si, respectively [70, 71].

Figure 14, Figure 15, Figure 16 and 17 shows the FTIR images for Neat-SiMn, NaOH-SiMn, HCl-SiMn, and H_2SO_4 -SiMn. It is noted that multiple peaks at 2000 - 2500 cm^{-1} was due to stretching vibration of Si-O and Si-Mn, which occurred in and out of phase for SiO for silicon manganese slag [70-72]. The alkaline treatment causes the peak almost diminished which shows the Si-Mn and Si-O structure were in plane, while acid caused the bending of Si-O and Si-Mn which at the end created rougher needle structure of silicon manganese slag [70-72]. In Figure 15, the peak at 977 to 1176 cm^{-1} was due to asymmetric and symmetric tetrahedral of SiO or stretch vibration of Al_2O_3 , whereas 977 cm^{-1} was due to vibration bending of Si-O-Si [71]. It also noted that H_2SO_4 had eliminated Na and Mg as shown by EDS/EDX and FTIR in Figure 10, Figure 17 and Table 8, which created the rough needle surface as shown in Figure 3(d).

4.0 Conclusions

In conclusion, the compressive strength of silicon manganese concrete (SMC) achieved concrete strength of 37.3 MPa and 51.1 MPa at 28th day for the SMC30 and SMC50, respectively which complied with Grade 30 and Grade 50 standards. Alkali and acid modified the neat silicon manganese slag structure as shown by SEM, whereas the alkaline treatment smoothen the structure and acid treatment roughen the surface of the silicon manganese slag. FTIR showed there are significant change in the functional group which caused stretching and vibration of Si-O and Si-Mn functional groups of silicon manganese slag due to modifications, while EDS significantly showed the high content of both silicon (Si) and manganese (Mn) elements. Therefore, it was concluded that curing duration increases the strength of SMC, which is useful for fully replacement of NWC

Declarations

ACKNOWLEDGEMENTS

The authors would like to thank and acknowledge Universiti Malaysia Sarawak (UNIMAS), Swinburne University of Technology Sarawak Campus, and OM Materials (Bintulu) Sdn. Bhd. for their support.

AUTHOR DECLARATIONS

The authors declare no competing interests.

ETHICS APPROVAL

Not applicable

CONSENT TO PARTICIPATE

Not applicable

CONSENT FOR PUBLICATION

Not applicable

AVAILABILITY OF DATA AND MATERIALS

Materials can be obtained from OM Materials Sdn. Bhd., Bintulu, Sarawak

FUNDING

Funding information is not applicable / No funding was received.

AUTHORS' CONTRIBUTIONS

Chin Mei Yun and Muhammad Khusairy Bin Bakrifabricated and carried out the experiment with support from Perry Law NyukKhui. Chin Mei Yun and Muhammad Khusairy Bin Bakri wrote the manuscript with support from Md. Rezaur Rahman, Kuok King Kuok and Perry Law NyukKhui.

References

1. Kim Y.J., Jeon, S.J., Choi, M.S., Kim, Y.J., Choi, Y.W.(2010), The Quality Properties of Self Consolidating Concrete using Lightweight Aggregate. In: Oh, B.H., Choi, O.C., Chung, L. (eds.) Fracture Mechanics of Concrete and Concrete Structures – High Performance, Fiber Reinforced Concrete, Special Loadings and Structural Applications, pp. 1342-1346. <https://framcos.org/FraMCoS-7/11-08.pdf>
2. Lotfabad, P. (2014), High-rise Buildings and Environmental Factors. Renewable and Sustainable Energy Reviews 38(1), 285-295. <https://doi.org/10.1016/j.rser.2014.05.024>
3. Rossignolo, J.A., Agnesini, M.V.C., Morais, J.A. (2003) Properties of High-performance LWAC for Precast Structures with Brazilian Lightweight Aggregates. Cement and Concrete Composites 25(1), 77-82. [https://doi.org/10.1016/S0958-9465\(01\)00046-4](https://doi.org/10.1016/S0958-9465(01)00046-4)
4. Chour, H.-B., Kim, J.M. (2020) Properties of Silicon Manganese Slag as An Aggregate for Concrete Depending on Cooling Conditions. Journal of Material Cycle and Waste Management 22(1), 1067-1080. <https://doi.org/10.1007/s10163-020-01003-8>
5. Yasar, E., Atis, C.D., Kilic, A., Gulsen, H. (2003) Strength Properties of Lightweight Concrete Made with Basaltic Pumice and Fly ash. Materials Letters 57(15), 2267-2270. [https://doi.org/10.1016/S0167-577X\(03\)00146-0](https://doi.org/10.1016/S0167-577X(03)00146-0)
6. Oliveira, R.W.H., Fernandes, G., Sousa, F.C., Barreto, R.A. (2017) Chemical and Mineralogical Characterization of Silicon Manganese Iron Slag as Railway Ballast. REM International Engineering Journal 7(4), 385-391. <https://doi.org/10.1590/0370-44672017700019>

7. Holm, T.A. (1994) Lightweight Concrete and Aggregates. In: Klieger, P., Lamond, J. (eds.). Significance of Tests and Properties of Concrete and Concrete-Making Materials, ASTM International, pp. 522-532.
<https://doi.org/10.1520/STP36447S>
8. Manju, K., Kumar, B.D., Kumar, S.S., Kumar, S.N. (2018) Behaviour of Concrete by Using Artificial Aggregates A Review. *International Journal of Engineering & Technology* 7(2.21) 255-258.
<https://doi.org/10.14419/ijet.v7i2.21.12183>
9. Frias, M., de Rojas, M.I.S., Santamaria, J., Rodriguez, C. (2006) Recycling of Silicomanganese Slag as Pozzolanic Material in Portland Cements: Basic and Engineering Properties. *Cement and Concrete Research* 36(3), 487-491.
<https://doi.org/10.1016/j.cemconres.2005.06.014>
10. Saxena, S., Tembhurkar, A.R. (2018) Impact of Use of Steel Slag as Coarse Aggregate and Wastewater on Fresh and Hardened Properties of Concrete. *Construction and Building* 165(1), 126-137.
<https://doi.org/10.1016/j.conbuildmat.2018.01.030>
11. Hainin, M.R., Yusoff, N.I.M., Sabri, M.F.M., Aziz, M.A.A., Hameed, M.A.S., Reshi, W.F. (2012) Steel Slag as an Aggregate Replacement in Malaysian Hot Mix Asphalt. *ISRN Civil Engineering*, 2012(1), 1-5
<https://doi.org/10.5402/2012/459016>
12. Ismail, S., How, K.W., Ramli, M. (2013) Sustainable Aggregates: The Potential and Challenge for Natural Resources Conservation. *Procedia – Social and Behavioral Science* 101(1), 100-109.
<https://doi.org/10.1016/j.sbspro.2013.07.183>
13. Nor, A.M., Yahya, Z., Abdullah, M.M.A.B., Razak, R.A., Ekaputri, J.J., Faris, M.A., Hamzah, H.N. (2016) A Review on the Manufacturing of Lightweight Aggregates Using Industrial By-Product. *MATEC Web of Conferences* 78(1), 1-8.
<https://doi.org/10.1051/mateconf/20167801067>
14. Sherly, R., Kumar, S.S. (2011) Valuable Products from Fly Ash - A Review. *Journal of Industrial Pollution Control* 27(2), 113-120. <http://www.icontrolpollution.com/articles/valuable-products-from-fly-ash-a-review-1-4.pdf>
15. Kumar, S., Singh, S.K., Mishra, S.C. (2018) Processing and Characterization of Fly-ash Compacts. *Materials Today: Proceedings* 5(2), 3396-3402. <https://doi.org/10.1016/j.matpr.2017.11.584>
16. Hashmi, A.F., Haq, M.u. (2018) Indian Based Fly Ash & International Based Fly Ash: A Review Paper. *IOP Conference Series: Materials Science and Engineering* 404(1), 1-5. <https://doi.org/10.1088/1757-899X/404/1/012035>
17. Ersoy, B., Kavas, T., Evcin, A., Baspinar, S., Sariisik, A., Dikmen, S. (2009) Production Of Fired Ceramic Materials from Fly Ash With Witherite Additive. *AfyonKocatepe University Journal of Science and Engineering Sciences* 9(3), 45-52. <https://dergipark.org.tr/tr/download/article-file/18735>
18. Kim, K.D., Kang, S.G. (2007) Manufacturing artificial lightweight aggregates using coal bottom ash and clay. *Journal of Korean Crystal Growth and Crystal Technology* 17(6), 277–282
<http://koreascience.kr/article/JAKO200706717302090.pdf>
19. Ruthkowska, G., Wichowski, P., Franus, M., Mendryk, M., Fronczyk, J. (2020) Modification of Ordinary Concrete Using Fly Ash from Combustion of Municipal Sewage Sludge. *Materials* 13(2), 487.
<https://doi.org/10.3390/ma13020487>
20. Sun, J.S., Kim, J.M., Sung, J.H. (2016) Evaluation on the applicability of dry processed bottom ash as lightweight aggregate for construction fields. *Journal of Material Cycles and Waste Management* 18(4), 752–762.
<https://doi.org/10.1007/s10163-015-0367-x>
21. Juenger MCG, Winnefeld F, Provis JL, Ideker JH (2011) Advances in alternative cementitious binders. *Cement and Concrete Research* 41(12), 1232–1243. <https://doi.org/10.1016/j.cemconres.2010.11.012>

22. Ferronato, N., Torretta, V. (2019) Waste Mismanagement in Developing Countries: A Review of Global Issues. *International Journal of Environmental Research and Public Health* 16(6), 1060.
<https://doi.org/10.3390/ijerph16061060>
23. Kambole, C., Paige-Green, P., Kupolati, W.K., Ndambuki, J.M., Adeboje, A. (2019) Comparison of technical and short-term environmental characteristics of weathered and fresh blast furnace slag aggregates for road base applications in South Africa. *Case Studies in Construction Materials* 11(1), 1-13.
<https://doi.org/10.1016/j.cscm.2019.e00239>
24. Neto, J.B.F., Faria, J.O.G., Fredericci, C., Chotoli, F.F., Silva, A.N.L., Ferraro, B.B., Ribeiro, T.R., Malynowskyj, A., Quarcioni, V.A., Lotto, A.A. (2015) Modification of Molten Steelmaking Slag for Cement Application. *Journal of Sustainable Metallurgy* 2(1), 13-27. <https://doi.org/10.1007/s40831-015-0031-7>
25. Yildirim, I.Z., Prezzi, M. (2011) Chemical, Mineralogical, and Morphological Properties of Steel Slag. *Advances in Civil Engineering* 2011(1), 1-14. <https://doi.org/10.1155/2011/463638>
26. Wang, H., Wang, Y., Cui, S., Wang, J. (2019) Reactivity and Hydration Property of Synthetic Air Quenched Slag with Different Chemical Compositions. *Materials* 12(6), 1-24. <https://doi.org/10.3390/ma12060932>
27. Altun, I.A., Yilmaz, I. (2002) Study on steel furnace slags with high MgO as additive in Portland cement. *Cement and Concrete Research* 32(8), 1247–1249. [https://doi.org/10.1016/S0008-8846\(02\)00763-9](https://doi.org/10.1016/S0008-8846(02)00763-9)
28. Rojas, M.F., Rojas, M.I.S. (2004) Chemical assessment of the electric arc furnace slag as construction material: Expansive compounds. *Cement and Concrete Research* 34(10), 1881–1888.
<https://doi.org/10.1016/j.cemconres.2004.01.029>
29. Kourounis, S., Tsivilis, S., Tsakiridis, P.E., Papadimitriou, G.D., Tsibouki, Z. (2007) Properties and hydration of blended cements with steelmaking slag. *Cement and Concrete Research* 37(6), 815–822. <https://doi.org/10.1016/j.cemconres.2007.03.008>
30. Frias M., Rojas, M.I.S., Santamaria, J., Rodriguez, C. (2006) Recycling of silico-manganese slag as pozzolanic material in Portland cements: Basic and engineering properties. *Cement and Concrete Research* 36(3), 487–491.
<https://doi.org/10.1016/j.cemconres.2005.06.014>
31. Choi, S., Kim, J., Oh, S., Han, D. (2017) Hydro-thermal reaction according to the CaO/SiO₂ mole-ratio in silico-manganese slag. *Journal of Materials Cycles and Waste Management* 19(1), 374–381.
<https://doi.org/10.1007/s10163-015-0431-6>
32. Patil, A.V., Pande, A.M. (2011) Behaviour of silico manganese slag manufactured aggregate as material for road and rail track construction. *Advanced Materials Research* 255(1), 3258–3262.
<https://doi.org/10.4028/www.scientific.net/AMR.255-260.3258>
33. Choi, S., Kim, J.-M., Han, D., Kim, J.-H. (2016) Hydration properties of ladle furnace slag powder rapidly cooled by air. *Construction and Building Materials* 113(1), 682–690. <https://doi.org/10.1016/j.conbuildmat.2016.03.089>
34. ASTM C494-19 (2019) Standard Specification for Chemical Admixtures for Concrete, ASTM International, West Conshohocken, PA. https://doi.org/10.1520/C0494_C0494M-19
35. BS 5075-1:1982 (1982) Concrete admixtures. Specification for accelerating admixtures, retarding admixtures and water reducing admixtures. British Standard.
36. IS 10262:2019 (2019) Concrete Mix Proportioning – Guidelines. Indian Standard.
37. ASTM E2015-04 (2014), Standard Guide for Preparation of Plastics and Polymeric Specimens for Microstructural Examination. ASTM International, West Conshohocken, PA. <https://doi.org/10.1520/E2015-04R14>
38. ASTM E2142-08 (2015), Standard Test Methods for Rating and Classifying Inclusions in Steel Using the Scanning Electron Microscope. ASTM International, West Conshohocken, PA. <https://doi.org/10.1520/E2142-08R15>

39. ASTM C1723-16 (2016), Standard Guide for Examination of Hardened Concrete Using Scanning Electron Microscopy. ASTM International, West Conshohocken, PA. <https://doi.org/10.1520/C1723-16>
40. ASTM E1508-12 (2019), Standard Guide for Quantitative Analysis by Energy-Dispersive Spectroscopy. ASTM International, West Conshohocken, PA. <https://doi.org/10.1520/E1508-12AR19>
41. ASTM E168-16 (2016), Standard Practices for General Techniques of Infrared Quantitative Analysis. ASTM International, West Conshohocken, PA. <https://doi.org/10.1520/E0168-16>
42. ASTM E1252-98 (2013), Standard Practice for General Techniques for Obtaining Infrared Spectra for Qualitative Analysis. ASTM International, West Conshohocken, PA. <https://doi.org/10.1520/E1252-98R13E01>
43. BS EN 196-1:2016 (2016) Methods of testing cement. Determination of strength. British Standard.
44. Ganesh, G., Ramesh K.V., Sudhakar, C., Jagadeesh, S. (2017), Influence of Silico Manganese Slag on Mechanical and Durability Properties of Concrete. International Journal of Civil Engineering and Technology (IJCIET), Vol 9 (7), 1597-1604. <http://www.iaeme.com/ijciyet/issues.asp?JType=IJCIET&VType=9&IType=7>
45. Balog, A.-A., Cobirzan, N., Mosonyu, E. (2014) Microstructural Analysis for Investigation of Limestone Damages – A Case Study of The Fortress Wall of Cluj-Napoca, Romania. Romanian Journal of Physics, 59(5-6), 608-613. http://www.nipne.ro/rjp/2014_59_5-6/0608_0613.pdf
46. Balog, A.-A., Cobirzan, N., Barbu-Tudoran, L. (2014) Evaluation of Limestone with Non-Invasive Analytical Methods. Romanian Journal of Physics, 59(5-6), 601-607. http://www.nipne.ro/rjp/2014_59_5-6/0601_0607.pdf
47. Johansson, S., Sparrenbom, Fiandaca, F. Lindskog, A., Olsson, P.-I., Dahlin, T., Rosqvist, H. (2017), Geophysical Journal International, 208(2), 954-972. <https://doi.org/10.1093/gji/ggw432>
48. Mounia, B., Merzoug, B., Chaoki, B., Djaouza, A.A. (2013) Physico-Chemical Characterization of Limestones and Sandstones in a Complex Geological Context, Example North-East Constantine: Preliminary Results. IACSIT International Journal of Engineering and Technology, 5(1), 114-118. <http://www.ijetch.org/papers/523-R029.pdf>
49. Liu, S., Yan, P. (2010) Effect of limestone powder on microstructure of concrete. Journal of Wuhan University of Technology – Materials Science Edition, 25(1), 328-331. <https://doi.org/10.1007/s11595-010-2328-5>
50. Chen, J.F., Sorelli, L., Vandamme, M., Ulm, F.-J., Chanvillard, G. (2010) A Coupled Nanoindentation/SEM-EDS Study on Low Water/Cement Ratio Portland Cement Paste: Evidence for C–S–H/Ca(OH)₂ Nanocomposites. Journal of the American Ceramic Society 93(5), 1484-1493. <https://doi.org/10.1111/j.1551-2916.2009.03599.x>
51. Awoyera, P.O., Olofinnade, O.M., Busari, A.A., Akinwumi, I.I., Oyefesobi, M., Ikemefuna, M. (2016) Performance of steel slag aggregate concrete with varied water-cement ratio. JurnalTeknologi 78(10), 125-131. <https://doi.org/10.11113/jt.v78.8819>
52. Anastasiou, E., Papayianni, I. (2006) Criteria for The Use of Steel Slag Aggregates in Concrete. In: Konsta-Gdoutos, M.S. (eds) Measuring, Monitoring and Modeling Concrete Properties. Springer, Dordrecht. https://doi.org/10.1007/978-1-4020-5104-3_51
53. Oliveira, R.W.H., Fernandes, G., Sousa, F.C., Barreto, R.A. (2017) Chemical and mineralogical characterization of silicon manganese iron slag as railway ballast. REM – International Engineering Journal 70(4), 385-391. <http://dx.doi.org/10.1590/0370-44672017700019>
54. Akbar, N.A., Aziz, H.A., Adlan, M.N. (2016) Potential of High Quality Limestone as Adsorbent for Iron and Manganese Removal in Groundwater. JurnalTeknologi 78(9-4), 77-82. <https://doi.org/10.11113/jt.v78.9700>
55. Awang, H., Ahmad, M.H., Al-Mulali, M.Z. (2015) Influence of Kenaf And Polypropylene Fibres on Mechanical and Durability Properties of Fibre Reinforced Lightweight Foamed Concrete. Journal of Engineering Science and Technology 10(4), 496-508.

[http://jestec.taylors.edu.my/Vol%2010%20issue%204%20April%202015/Volume%20\(10\)%20Issue%20\(4\)%20496-%20508.pdf](http://jestec.taylors.edu.my/Vol%2010%20issue%204%20April%202015/Volume%20(10)%20Issue%20(4)%20496-%20508.pdf)

56. Lee, S.-T., Park, D.-W., Ann, K.-Y. (2008) Mitigating effect of chloride ions on sulfate attack of cement mortars with or without silica fume. *Canadian Journal of Civil Engineering* 35(11), 1210-1220. <https://doi.org/10.1139/L08-065>
57. Dawood, E.T., Ramli, M. (2012) Properties of High-Strength Flowable Mortar Reinforced with Palm Fibers. *International Scholarly Research Notices*. *International Scholarly Research Notices*. 2012(1), 1-5. <https://doi.org/10.5402/2012/718549>
58. Cao, M., Ming, X., He, K., Li, L., Shen, S. (2019) Effect of Macro-, Micro- and Nano-Calcium Carbonate on Properties of Cementitious Composites—A Review. *Materials* 12(5), 781. <https://doi.org/10.3390/ma12050781>
59. Kelestermur, O., Yildiz, S. (2006) Effect of Various NaCl Concentration on Corrosion of Steel in Concrete Produced by Addition of Styrofoam. *Gazi University Journal of Science* 19(3), 163-172. <https://dergipark.org.tr/tr/download/article-file/83098>
60. Prucker, F., Gjør, O.E. (2004) Effect of CaCl₂ and NaCl additions on concrete corrosivity. *Cement and Concrete Research* 34(7), 1209-1217. <https://doi.org/10.1016/j.cemconres.2003.12.015>
61. Quraishi, M.A., Nayak, D.K., Kumar, D., Kumar V. (2017) Corrosion of Reinforced Steel in Concrete and Its Control: An overview. *Journal of Steel Structures & Construction*. 3(1). 1-6. <https://doi.org/10.4172/2472-0437.1000>
62. Bertolini, L., Carsana, M., Gastaldi, M., Lollini, F., Redaelli, E. (2016) Corrosion of Steel in Concrete and Its Prevention in Aggressive Chloride-Bearing Environments. 5th International Conference on Durability of Concrete Structures, 13-25. <https://docs.lib.purdue.edu/cgi/viewcontent.cgi?article=1153&context=icdcs>
63. Steenkamp, J.D., Maphutha, P., Makwarela, O., Banda, W.K., Thobadi, I., Sitefane, M., Gous, J., Sutherland, J.J. (2018) Silicomanganese production at Transalloys in the twenty-tens. *Journal of the Southern African Institute of Mining and Metallurgy* 118(3), 309-320. <http://dx.doi.org/10.17159/2411-9717/2018/v118n3a13>
64. Jagadeesh, S., Ramesh, K.V., Ganesh, S., Kumar, D.S.S. (2018) Study on Tensile Strength Properties of Recycled Aggregate Concrete with and without Pozzolanic Materials. *International Journal of Civil Engineering and Technology (IJCIET)* 9(11), 671-679. <http://www.iaeme.com/ijciet/issues.asp?JType=IJCIET&VType=9&IType=11>
65. Ringdalen, E., Gaal, S., Tangstad, M., Ostrovski, O. (2010) Ore Melting and Reduction in Silicomanganese Production. *Metallurgical and Materials Transactions B* 41(1), 1220-1229. <https://doi.org/10.1007/s11663-010-9350-z>
66. Al-Degs, Y.S., El-Barghouthi M.I., Issa A.A., Khraisheh M.A., Walker G.M. (2006) Sorption of Zn(II), Pb(II), and Co(II) using natural sorbents: equilibrium and kinetic studies. *Water Research* 40(14), 2645 <https://doi.org/10.1016/j.watres.2006.05.018>
67. Preeti, S.N., Singh, B.K. (2007) Instrumental characterization of clay by XRF, XRD and FTIR. *Bulletin of Materials Science* 30(1), 235-238. <https://doi.org/10.1007/s12034-007-0042-5>
68. Gunasekaran, S., Anbalagan, G. (2007). Spectroscopic Characterization of Natural Calcite Minerals. *Spectrochimica Acta Part A: Molecular and Biomolecular Spectroscopy* 68(3), 656-664. <https://doi.org/10.1016/j.saa.2006.12.043>
69. Hajjaji, M., Kacim, S., Alami, A., El Bouadili, A., El Mountassir, M. (2001) Chemical and mineralogical characterization of a clay taken from the Moroccan Meseta and a study of the interaction between its fine fraction and methylene blue. *Applied Clay Science* 20(1-2), 1-12. [https://doi.org/10.1016/S0169-1317\(00\)00041-7](https://doi.org/10.1016/S0169-1317(00)00041-7)
70. Wang, Y.g, Han, F.-l., Zhao, S.-z., Mym H.-q (2017) Preparation and characterization of Manganese Slag and Fly Ash-based Geopolymer. *MATEC Web of Conferences* 130(1), 1-4. <https://doi.org/10.1051/mateconf/201713004006>

71. Xing, X., Pang, Z., Zheng, J., Du, Y., Ren, S., Ju, J. (2020) Effect of MgO and K₂O on High-Al Silicon-Manganese Alloy Slag Viscosity and Structure. *Minerals* 10(9), 810. <https://doi.org/10.3390/min10090810>
72. Andres, E.S., Prado, A.D., Martinez, F.L., Martil, I. (2000) Rapid thermal annealing effects on the structural properties and density of defects in SiO₂ and SiN_x:H films deposited by electron cyclotron resonance. *Journal of Applied Physics* 87(1187), 1-10. <https://doi.org/10.1063/1.371996>

Figures

Figure 1

The compressive strength of NWC and SMC.

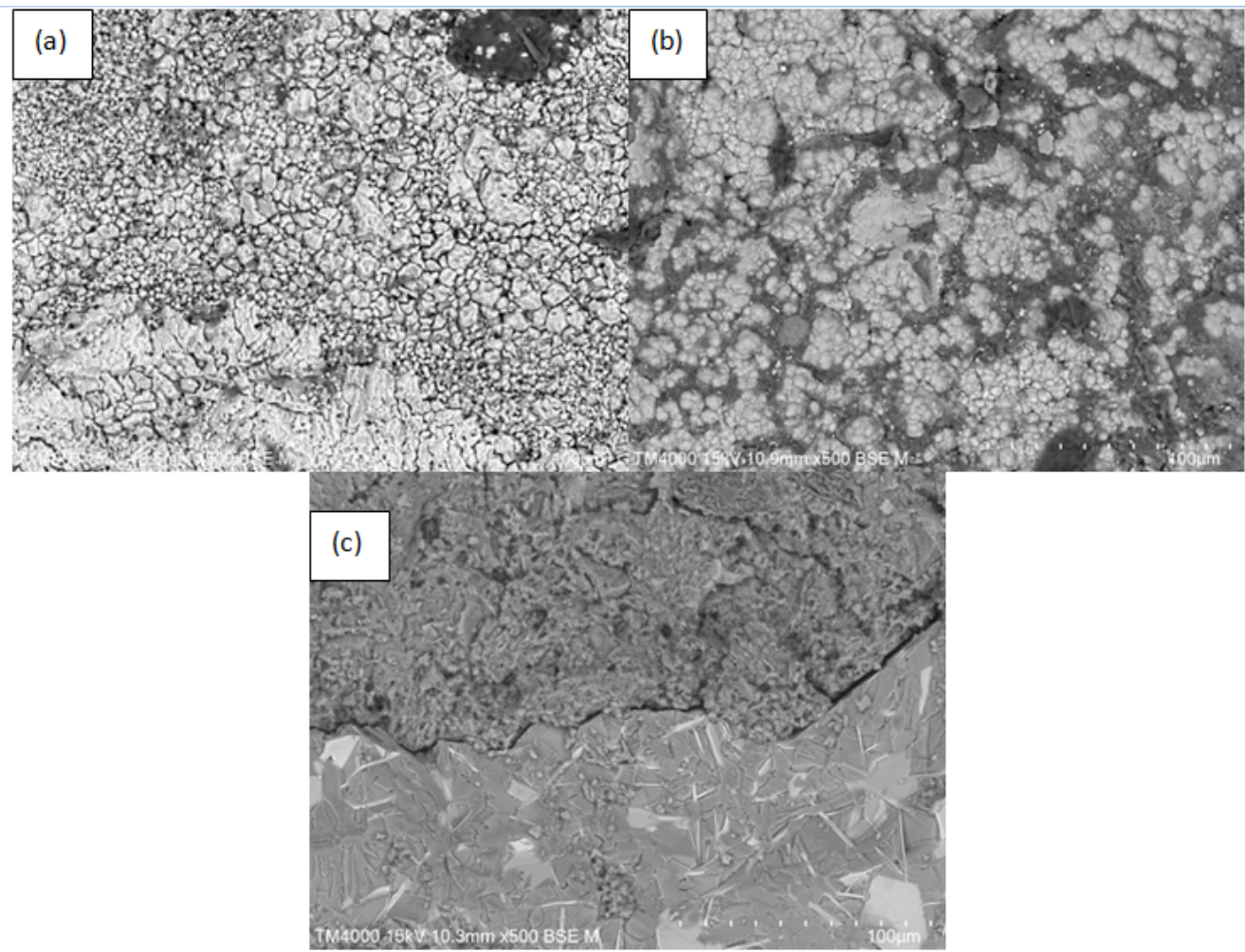


Figure 2

The SEM images at 500x magnification for (a) limestone, (b) ordinary Portland cement, and (c) silicon manganese concrete (SMC).

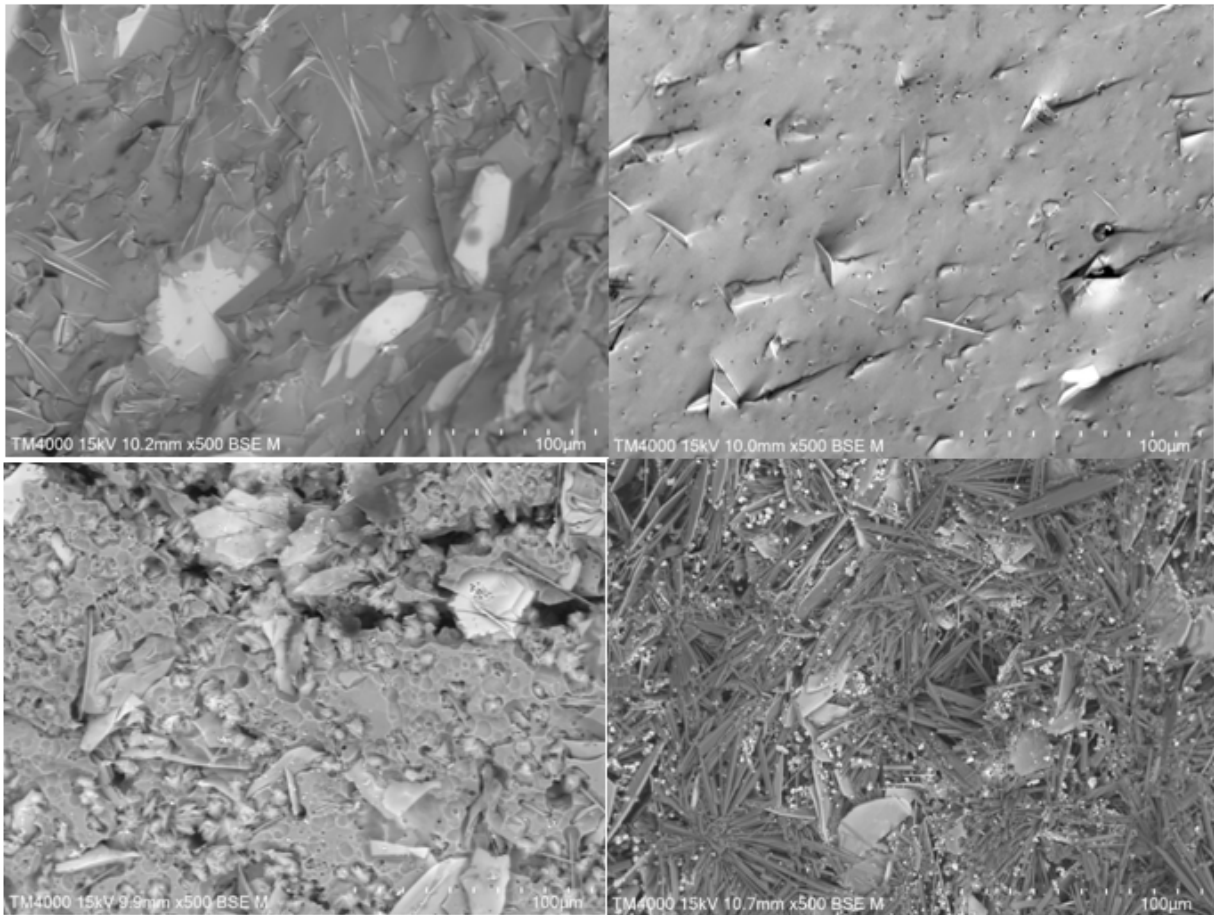


Figure 3

The SEM images at 500x magnification for (a) Neat-SiMn, (b) NaOH-SiMn, (c) HCl-SiMn, and (d) H₂SO₄-SiMn

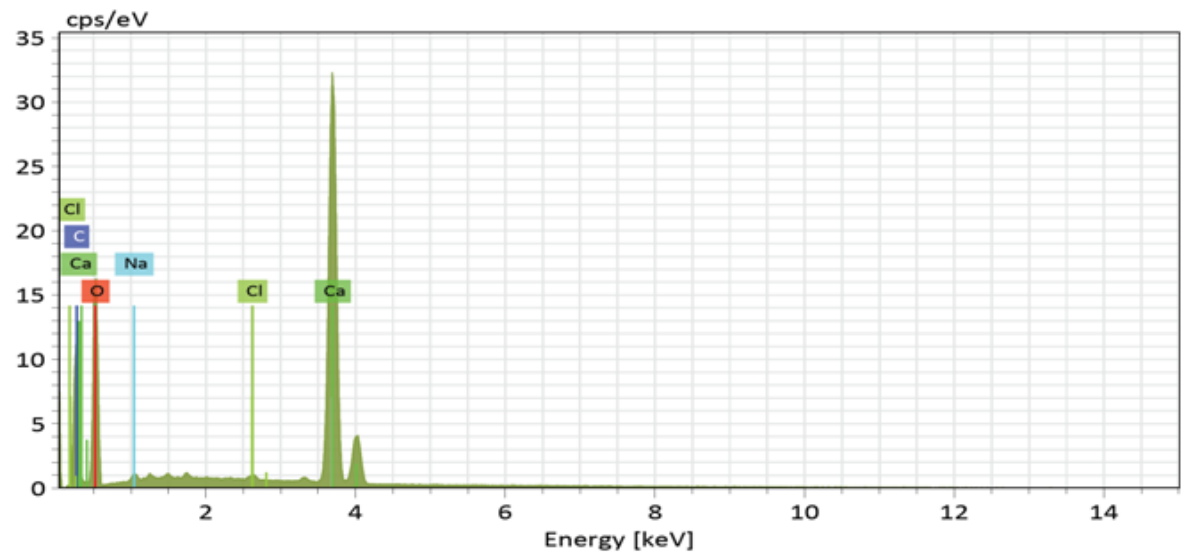


Figure 4

EDS spectrum graph of limestone

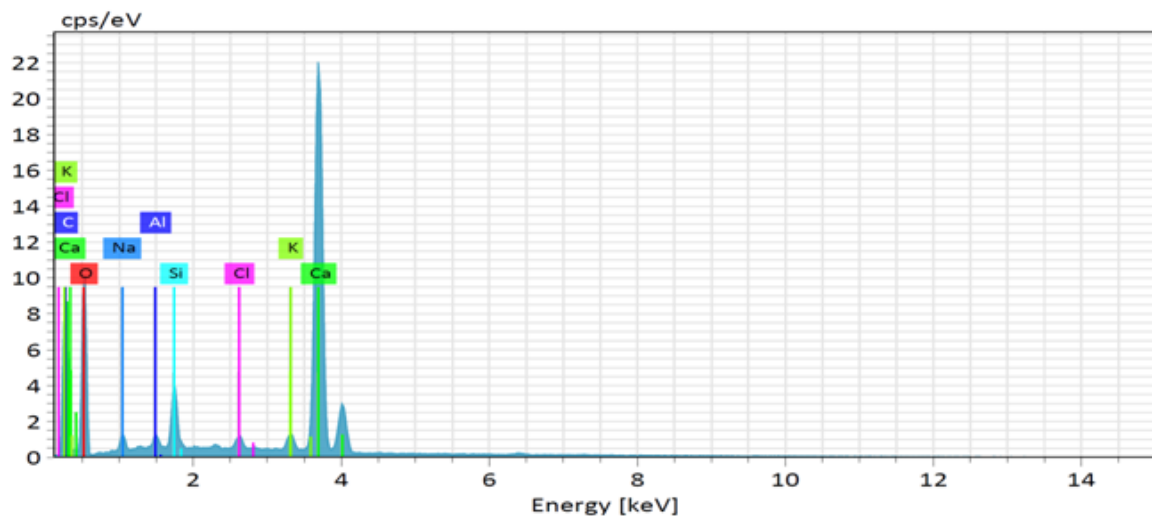


Figure 5

EDS spectrum graph of ordinary Portland cement

Figure 6

EDS spectrum graph of silicon manganese cement (SMC).

Figure 7

EDS spectrum graph of Neat-SiMn

Figure 8

EDS spectrum graph of NaOH-SiMn

Figure 9

EDS spectrum graph of HCl-SiMn

Figure 10

EDS spectrum graph of H₂SO₄-SiMn

Figure 11

FTIR spectrum graph for limestone

Figure 12

FTIR spectrum graph for ordinary Portland cement (OPC).

Figure 13

FTIR spectrum graph for silicon manganese concrete (SMC).

Figure 14

FTIR spectrum graph for Neat-SiMn

Figure 16

FTIR spectrum graph for HCl-SiMn

Figure 17

FTIR spectrum graph for H₂SO₄-SiMn